

Quiet Sun Explosive Events: Jets, Splashes, and Eruptions

D. E. Innes · L. Teriaca

© Springer ●●●

Abstract Explosive events are broad non-Gaussian wings in the line profiles of small transition region phenomena. Images from the Solar Dynamics Observatory (SDO) give a first view of the plasma dynamics at the sites of explosive events seen in O VI spectra of a region of quiet Sun, taken with the ultraviolet spectrometer SUMER/SOHO. Distinct event bursts were seen either at the junction of supergranular network cells or near emerging flux. Three are described in the context of their surrounding transition region (304Å) and coronal (171Å) activity. One showed plasma ejections from an isolated pair of sites, with a time lag of 50 s between events. At the later site, the EUV images show a hot core surrounded by a small, expanding ring of chromospheric emission which we interpret as a ‘splash’. The second explosive event burst was related to flux cancellation, inferred from SDO/HMI magnetograms, and a coronal dimming surrounded by a ring of bright EUV emission with explosive events at positions where the spectrometer slit crossed the bright ring. The third series of events occurred at the base of a slow mini-CME. All events studied here imply jet-like flows probably triggered by magnetic reconnection at supergranular junctions. Events come from sites close to the footpoints of jets seen in AIA images, and possibly from the landing site of induced high velocity flows. They are not caused by rapid rotation in spicules.

Keywords: Transition region; Magnetic reconnection, Observational Signatures

1. Introduction

Although transition region explosive events are seen very frequently in spectra of the quiet and active Sun, images of their sites have been difficult to obtain until recently. Transition region explosive event is the name given to small (1-5 arcsec), short-lived (1-5 min) non-Gaussian broadenings in the wings of spectral lines formed around 10^5 K. They were discovered in HRTS spectra of transition region lines by Brueckner and Bartoe (1983) and later described in more detail by Dere, Bartoe, and Brueckner (1989) and Dere (1994). Since

Max-Planck Institut für Sonnensystemforschung,
Max-Planck-Str. 2, 37191 Katlenburg-Lindau email:
innes@mps.mpg.de email: teriaca@mps.mpg.de

the launch of SUMER/SOHO explosive events have been seen regularly in lines with formation temperature 6×10^4 K (*e.g.* C III) to 7×10^5 K (*e.g.* Ne VIII) (Wilhelm *et al.*, 2007). Both extended red and/or blue wings are observed. Analysis of the line asymmetry shows a change with ion, position and evolution (Dere, Bartoe, and Brueckner, 1989; Winebarger *et al.*, 2002; Mendoza-Torres, Torres-Papaqui, and Wilhelm 2004) and often a spatial offset between the red and blue wings. Events often come in bursts (Innes *et al.*, 1997b) with 3-5 min between consecutive events (Ning, Innes, and Solanki, 2004).

The evolution of line profiles across individual events shows that in some events the underlying flows are similar to bi-directional jets (Innes *et al.*, 1997a) originating in the transition region and ejected down to the chromosphere and up towards the corona. Examples have also been found that resemble supersonic up and down flows along loops (Teriaca *et al.*, 2004) and, at the limb, flows along macropicules (Wilhelm, 2000). Analysis of the energetics of the flows suggests that they carry equal energy in both directions (Winebarger *et al.*, 2002). The energy input sites do not move during the course of the events but expand and shrink slowly across the surface with a speed about 25 km s^{-1} (Ning, Innes, and Solanki, 2004).

Explosive events seem to concentrate along the boundaries of the magnetic network near sites of cancelling/evolving magnetic flux (Porter and Dere, 1991; Chae *et al.*, 1998; Muglach, 2008; Aiouaz, 2008) and are thus believed to result from magnetic reconnection at the Sun. Although the line profiles, energetics and magnetic field evolution can be explained by energy release at a reconnection site in the transition region (Sterling, Shibata, and Mariska, 1993; Dere *et al.*, 1991; Innes *et al.*, 1997a; Innes and Tóth, 1999; Roussev *et al.*, 2001), it has been argued that the transition region reacts with similar signatures of explosive energy release to microflaring in the corona (Krucker and Benz, 2000) or reconnection in the photosphere (Tarbell *et al.*, 1999; Ryutova and Tarbell, 2000). It is also possible that explosive events are related to chromospheric jets that cause jet-like brightenings in transition region and coronal images (De Pontieu *et al.*, 2011). At the moment, the debate is still open as to where the primary energy input site is and can probably only be resolved by high resolution simultaneous spectroscopic imaging from the chromosphere to the corona.

An alternative to the jet/flow explanation is that the red and blue shifts are due to rotation rather than up and downflows (Curdt and Tian, 2011). Rotation is the explanation often given for observations of a red-to-blue change in Doppler shift during raster observations of spicules seen at the limb (Pike and Mason, 1998; Kamio *et al.*, 2010); however Xia *et al.* (2005) noticed similar red-to-blue changes in line profiles obtained during sit-and-stare observations of limb spicules. These are most simply explained as ejected plasma that reaches a certain height and then falls back along the same path, casting some doubt on the rotation interpretation. A more compelling argument against rotation as a general explanation for explosive events, particularly in disk center observations, is that nearly all observed off-limb jets/spicules have higher vertical than lateral velocities (Suematsu *et al.*, 2008; Scullion *et al.*, 2009; De Pontieu *et al.*, 2012), and it is unlikely that events seen at disk center will behave differently and exhibit faster rotation than outflow. In order to distinguish jet-like from swirling motion co-temporal images of the chromosphere, corona and spectra of explosive events like the ones reported here are very useful.

Much has been written about the association of flows, observed as Doppler shifted emission, with coronal brightenings particularly since the CDS/SOHO spectrometer generally saw brightenings without significant line broadening (Harrison, 1997; Harrison *et al.*, 1999; Harrison *et al.*, 2003; Madjarska and Doyle, 2003) and SUMER observing at higher resolution saw bursts of explosive events associated with brightenings (Innes, 2001; Brković and Peter, 2004). Quiet Sun brightenings at transition region temperatures can be due to many processes (Priest, Hood, and Bewsher, 2002) and this makes their interpretation confusing. For example, brightenings have been associated with eruption at network junctions where mixed-polarity fields are swept-up by supergranular flows (Harrison, 1997; Potts, Khan, and Diver, 2007; Innes *et al.*, 2009) and also with flux emergence (Doyle, Roussev, and Madjarska, 2004; Subramanian *et al.*, 2008). Innes (2001) showed that strong explosive events often had jet-like structure in TRACE C IV images but the TRACE 171Å quiet Sun emission was weak and difficult to interpret. In active regions strong explosive events have been seen to coincide with sites of 171Å brightenings at the footpoints and along H α jets (Madjarska, Doyle, and de Pontieu, 2009).

Now with Atmospheric Imaging Assembly (AIA) (Lemen *et al.*, 2012) images from the Solar Dynamics Observatory (SDO) we have much higher quality filter images of the sites of explosive events at both transition region and coronal temperatures, as well as high cadence line-of-sight magnetic field observations and continuum images that allow us to track the photospheric flows in which the magnetic flux is entrained.

The question to be addressed here is the structure and magnetic environment of brightenings associated with transition region explosive events. In the next section we describe the observations and give an overview of the quiet Sun region and sites of events. We then describe three explosive event bursts showing in each case how they relate to brightening in 304 and 171Å, the underlying magnetic field and photospheric flows.

2. Observations

The Solar Ultraviolet Measurements of Emitted Radiation (SUMER) spectrometer (Wilhelm *et al.*, 1995; Wilhelm *et al.*, 1997; Lemaire *et al.*, 1997) observed the O VI 1032Å line near disk center in sit-and-stare mode from 22:11 UT 28 June 2010 to 00:11 UT 29 June 2010 through the 4×300 arcsec² slit with a cadence of 60 s. The Sun's rotation rate at the position of the slit was 0.15 arcsec min⁻¹, so over the two hours SUMER observed a region 18×300 arcsec². Chromospheric (304Å), lower coronal (171Å), line-of-sight magnetic field, and supergranular flow images of the observed region are shown in the four panels of Figure 1. The explosive events are discussed in the context of these four observables obtained from the AIA and Helioseismic and Magnetic Imager (HMI) (Scherrer *et al.*, 2012) on SDO.

During our observations the O VI line was dispersed on the bare part of detector B. After each 60 s exposure 100 pixels across the O VI line were transmitted to the ground. This corresponds to a spectral window of 4.4Å or ± 600 km s⁻¹ in line Doppler shift. After decompression, the SUMER data have been corrected

for dead time losses, local gain depression, flat-field and geometric distortion using the standard software provided in SolarSoft. The best available flatfield was obtained almost one year after the time of these observations. Since the flatfield evolves with time and position on the detector, we are unable to remove all flatfield artifacts. Residuals from the flatfield subtraction lead to stripes in maps of fitted parameters (*e.g.*, line width, see Figure 2). We checked their effect on the line profiles and found it to be modest. The SUMER detectors also have some small physical defects (damaged MCP) that cannot be corrected. Spectra from these locations are unreliable and not considered. Finally, it is important to mention that count rates in excess of 50 counts s^{-1} can produce irreversible gain depression, and thus alter the spectral profiles. This situation arises during the second event studied, where the line center count rates are high. However, careful inspection of the raw data reveals that the explosive event signature in the wings can be trusted.

AIA takes full Sun images with a spatial resolution of $0.6 \text{ arcsec pixel}^{-1}$ and time cadence of 12 s in 10 wavelength bands, including seven extreme ultraviolet (EUV), two ultraviolet and one visible filter. For the SDO analysis, we select two channels: 304\AA which is dominated by the He II lines formed around $5 \times 10^4 \text{ K}$ and 171\AA which is centered on the Fe IX line formed around $6 \times 10^5 \text{ K}$. The level 1 data have been processed to deconvolve the point spread function and then registered to level 1.6 using SolarSoft routines.

The underlying magnetic field and its evolution is obtained from HMI line-of-sight magnetograms with a pixel size 0.5 arcsec . Supergranule lanes and junctions are obtained by tracking the horizontal photospheric flows in HMI continuum images, taken with a cadence of 45 s. Flow velocities have been computed with the balltracking method developed by Potts, Barrett, and Diver (2004) (see also Attie, Innes, and Potts (2009)). First the continuum images are de-rotated to the same time, then tracking is done on individual granules in consecutive images. Supergranule flows are computed by smoothing the resultant velocities over a Gaussian width of 4 arcsec , and averaging over 45 min. The positions of the flow arrows shown in the figures have been computed by integrating arrow positions along streamlines. New arrows are continually added at random positions where there are few arrows and removed from regions where they cluster together. Arrows collect where the flows converge along supergranular cell boundaries and at junctions. Thus the arrows in Figure 1d mostly overlies the magnetic field concentrations, except where flux emergence has occurred (yellow circle).

The contribution function of the O VI 1032 line peaks at about $3 \times 10^5 \text{ K}$ and has a tail extending to higher temperatures. For this reason the O VI matches both the 304\AA and 171\AA structures fairly well. Although the O VI formation temperature is closest to that of Fe IX, the transition region dynamics are better reflected in the 304\AA images and these are therefore used for coalignment with SUMER. In Figure 2, we have created a synthetic sit-and-stare 304\AA image of the region covered by the SUMER slit. For each SUMER exposure we have taken the 304\AA image closest to the central time and then binned the data over 4 arcsec in the X direction and 1 arcsec in the Y direction to give the same spatial coverage as the SUMER slit. There is very good overall agreement, and the alignment is within one arcsec in both directions. The main discrepancies are

where there are small brightenings in the O VI (e.g the brightening labelled ‘1’). As shown in the next section, these probably arise because the main brightening is very quick and not present in the 304Å image taken to represent the 1 min SUMER exposure. For coalignment, we find it sufficient to use one AIA image per minute.

An example of coaligned SUMER stigmatic spectra with the cotemporal AIA 304Å image is shown in Figure 3. As indicated by the horizontal dashed lines, explosive events coincide with brightening in the 304Å image. This was true for the whole time series, shown in the accompanying movie AIA_SUMER. It is also apparent from the movie that explosive events occur at specific sites and come in bursts. Strong events appear as profiles with widths greater than 80 km s^{-1} . In Figure 2c, we show the O VI Doppler widths and enclose explosive events bursts in black rectangles. The grouping has been made by inspection and based on the temporal and spatial proximity of events. A single event is one or more consecutive event profiles at a single site. If several neighbouring sites produce an explosive event, or if explosive events come and go at a single site then we call this an explosive event burst.

3. Event evolutions

All explosive events seen in O VI were associated with small-scale brightenings in the AIA 304Å images. Most events occurred in bursts but there were also several single or paired events. There were four main bursts. Unfortunately the two northern ones were near the detector defect and so are excluded from further study. We note that these bursts were just east of the newly emerged flux (Figure 1d). In the following section we show the environment around the other two bursts and the brightest of the event pairs to give a feel for the type of structure producing explosive events.

3.1. Jets and splash at loop footpoints

This isolated pair of explosive events (‘1’ in Figure 2) was associated with a pair of EUV brightenings that occurred in an otherwise quiet region, and allows a clear view of the individual explosive event sites. The evolution shown in Figures 4 and 5 only lasted three min. Each row shows the five AIA images from the 171Å (Figure 4) or 304Å (Figure 5) channel taken during the 60 s SUMER exposure, shown on the right. The 304Å images are taken 3 s after the 171Å ones. SUMER stigmatic images are shown on the right of the 171Å images and the line profiles at the sites of brightening on the right of the 304Å images.

In the AIA images, there are basically two small brightenings. They are seen as a well-separated pair in the first three frames along the middle row. The event started around 22:42:11 UT (the fourth frame on the top row) when both sites appear. The northern one is clearly the brightest and remained so for the first ~ 50 s. Then it faded and has disappeared in the 22:43:11 UT frame. As the northern site faded, the intensity at the southern site started to increase and reached its peak brightness at 22:43:35 UT (first frame on the bottom row). We

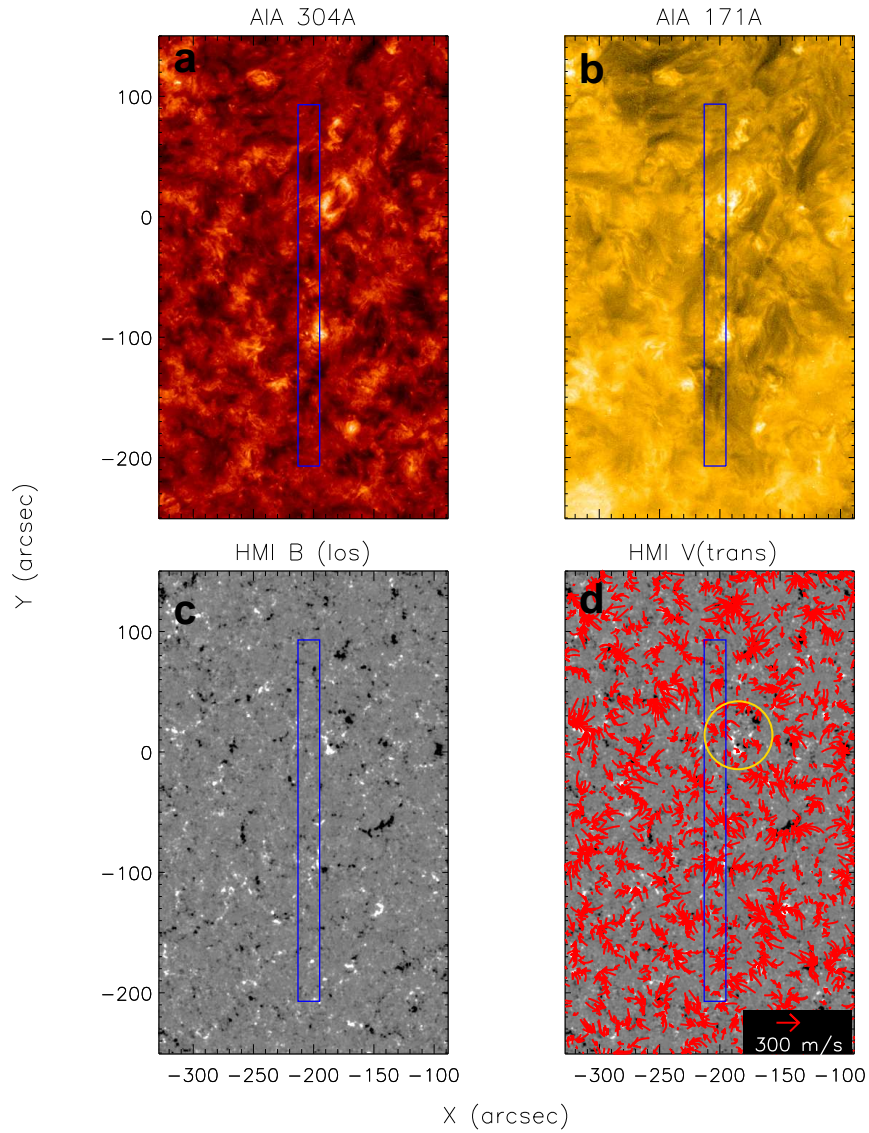


Figure 1. The region observed 2010 June 28 22:11:00 UT: a) 304Å; b) 171Å; c) line-of-sight magnetic field, scaled between ± 50 G; d) magnetic field with photospheric transverse flow arrows overplotted. The blue rectangle outlines the region covered by SUMER sit-and-stare observations. The yellow circle in (d) encloses a small site of recent flux emergence.

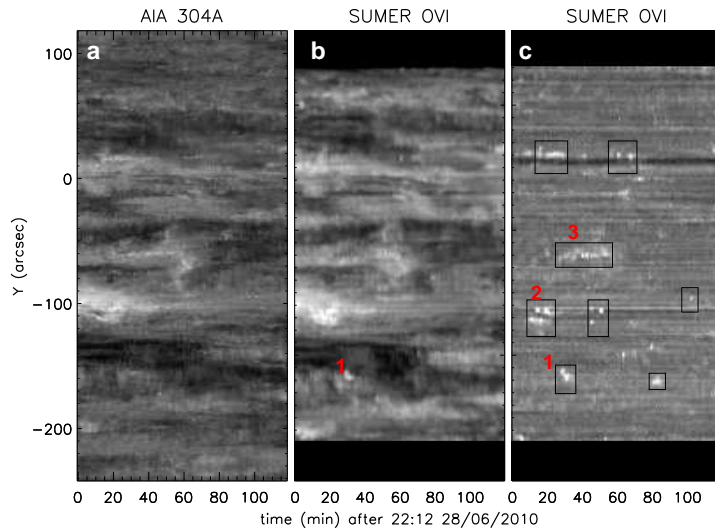


Figure 2. Coaligned AIA 304Å and SUMER O VI time series: (a) 304Å intensity; (b) O VI 1032Å intensity; (c) O VI 1032Å Doppler width scaled below 80 km s^{-1} . In (c), events bursts are enclosed with black rectangles. The ones discussed in the text are numbered. The horizontal stripes in (c) are artifacts due to imperfect flatfielding, with the exception of the larger one around solar $Y=10$, that is due to an MCP defect.

note that both sites produced explosive events in sync with the AIA brightenings. Initially only the northern site produced an explosive event (top row), then both (middle row) and at the end an explosive event was at the southern site only (bottom row).

The southern site has a distinctly different structure in the 171Å and 304Å images. The 304Å channel shows a small ring of bright emission with a dark center, while the 171Å channel shows a small bright point that coincides with the dark center of the 304Å ring (blue circles, Figures 4 and 5). Initially the 304Å ring is only 1-2 pixels (800 km) wide but over the following two images (30 s), the diameter doubles (first three frames in the bottom row, Figure 5).

The magnetic field evolution and supergranular flows, depicted as arrows, are shown in Figure 6. This was a small, almost unipolar (negative) supergranular junction. There was very little magnetic field evolution for the 2 hours around the event. HMI magnetograms have a 1σ noise level of 10 G (Liu *et al.*, 2012) so there may be weak positive polarity fields present.

The structure of the event suggests that this may have been a small magnetic loop. In particular because the 171Å emission connects the two brightenings in the frame at 22:42:23 UT (Figure 4 right hand image on the top row). Assuming a semi-circular loop, the length would have been about 5 Mm. At onset (22:42:11 UT) both sites appeared in the same 171 or 304Å image. We checked the EUV images from other channels and found that the two sites always appeared in the same image. Initially only the northern one produced jet-like flows. The travel time for a plasma jet with the observed velocity, $\sim 100 \text{ km s}^{-1}$, from

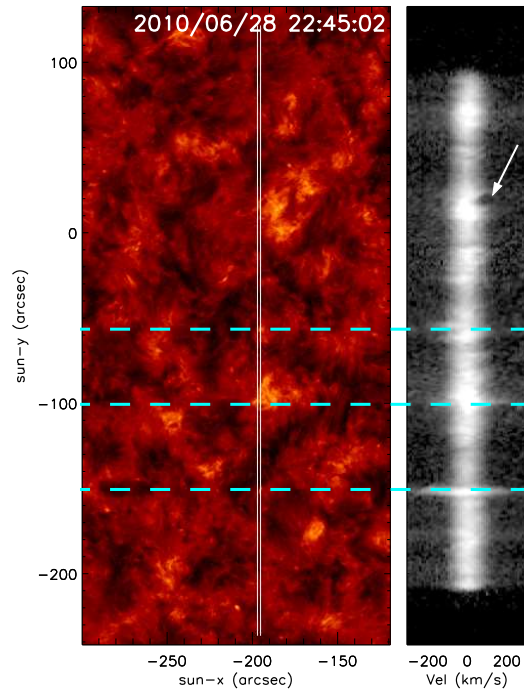


Figure 3. AIA 304Å structure around SUMER O VI explosive events: left) 304Å intensity; right) O VI 1032Å stigmatic spectrum. All three explosive events align with 304Å brightenings (dashed lines). The white arrow points to a detector defect. This is one frame from the accompanying movie AIA_SUMER.

one footpoint to the other would have been 50 s which is about the time between the fading of the northern footpoint and the peak intensity of the southern one. There was also a delay between the northern and southern explosive events. Due to the 60 s exposure time of SUMER, it is not possible to determine how long it was but it seems reasonable to assume it followed the brightening of the two footpoints.

A jet-like flow along a loop may explain the hot core surrounded by a ring of cooler emission seen at the other footpoint because high velocity plasma may create a splash when hitting the surface. It is not clear how much energy will be dissipated at the landing site. 1-D numerical simulations of plasmoid ejections along loops show that reflection can occur at the landing site (Sterling *et al.*, 1991). In 3-D, the situation is likely to be similar but the extra dimensions may give rise to splashes. Reverse jets have also been seen on a larger scale in X-ray images (Strong *et al.*, 1992; Shimojo *et al.*, 2007).

The bright core was also seen in 211 and 193Å images therefore it probably reached temperatures at least as high as 2 MK. Hot plasma is sometimes seen at the base of surges and jets (Madjarska, Doyle, and de Pontieu, 2009), so it

is also possible that the ring of chromospheric emission is the response of the surrounding plasma to a rapid surge-like up- and downflow.

3.2. Flux cancellation at supergranular junction

This burst of explosive events, labelled ‘2’ in Figure 2, extended over 20 arcsec, and was seen as the the bright patch of network near (-200,-100) in Figure 1 drifted westward under the SUMER slit. At this site, there were multiple 304Å brightenings and dimmings (see the movie AIA_SUMER). Especially at the time that the region was scanned by the SUMER slit, there were several sudden 304Å dimmings with a bright ring around their edge. The biggest such dimming was associated with this burst of explosive events, and is illustrated by snapshots of 304Å, 171Å and 171Å base difference images in Figure 7. Unlike the structure described in ‘1’, the central dimming and outer ring were seen simultaneously at 171Å, as well as at 193 and 211Å (not shown). We note that explosive event sites, indicated with arrows, are where the slit overlaps with the bright ring.

The ring-like structure suggests eruption of a small loop system with connections in all directions. Such an eruption would explain the explosive events along the ring’s edge since this is where one expects the footpoints of the erupting loops. Due to the 60 s time cadence, and sit-and-stare observing sequence, the explosive event structure cannot be resolved. They could be caused by bi-directional jets (Innes *et al.*, 1997a) or flows along small loops. The important point here is that they coincide with brightenings along the edge of the erupting ring so are flows not rotating spicules.

As seen in Figure 8 and the movie EVENT2_HMI, the event occurred at a mixed-polarity junction where converging flows were driving flux cancellation (yellow circles). Above we noted that the evolution looked like the opening of a small loop system and in Figure 7 one sees that initially there was a bright 304Å strand running southwards from the cancelling flux region. Eruption of this strand seems to have been the cause of the larger dimming. The actual dynamics of the eruption was probably more complicated than reconnection at a loop footpoint leading to eruption because there was a lot of surrounding small-scale activity but it may describe the essential process. Thus this event is a good example of flux cancellation leading to eruption and plasma jets in the transition region at the footpoints of an erupting loop system.

3.3. Explosive events at the base of a mini-CME

This series of explosive events, labelled ‘3’ in Figure 2, occurred at the onset site of a quiet Sun mini-CME. The eruption is best seen in the accompanying movies EVENT3_304 and EVENT3_171. It started at a small mixed polarity supergranular junction and propagated across the supergranular cell to the north east (see blue circles in Figures 9 and 11). The eruption is small compared with examples of mini-CMEs in the literature (Innes *et al.*, 2009; Podladchikova *et al.*, 2010; Zheng *et al.*, 2011). It was the largest crossed by the slit in the two hours of observation. Significant explosive events are only seen at the base of the mini-CME where the 304Å brightens, not where the propagating front moves along the slit.

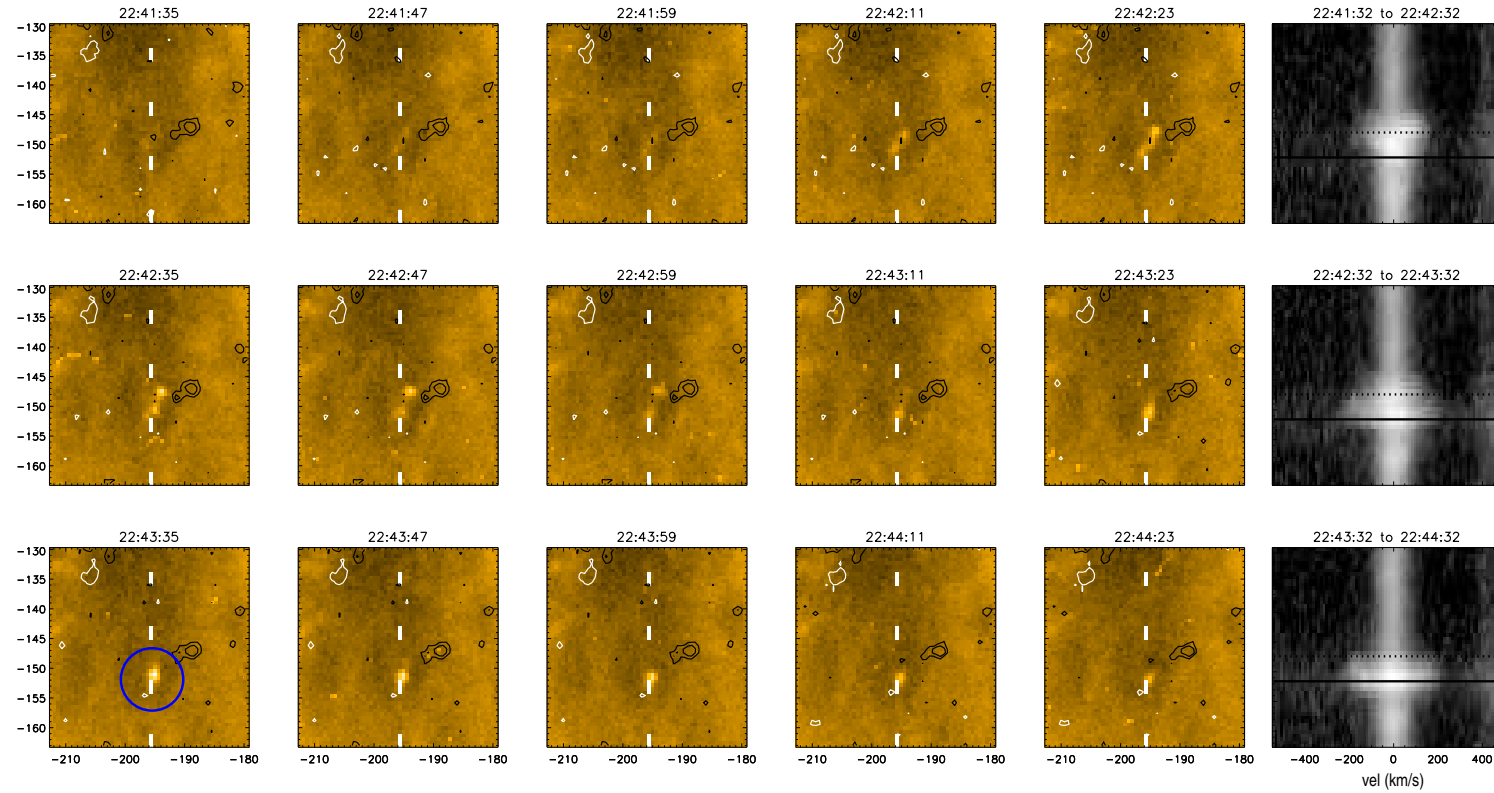


Figure 4.: The five 171Å AIA images along each row shows the evolution during the SUMER O VI exposure on the right. The vertical light blue dashed line in the middle of each 171Å image indicates the position of the SUMER slit. Line-of-sight magnetic field contours at $\pm 20, 50$ G are overplotted in white/black. On the SUMER spectra horizontal black solid and dotted lines indicate the position of the profiles shown in Figure 5. The blue circle in the bottom row surrounds the ‘splash’.

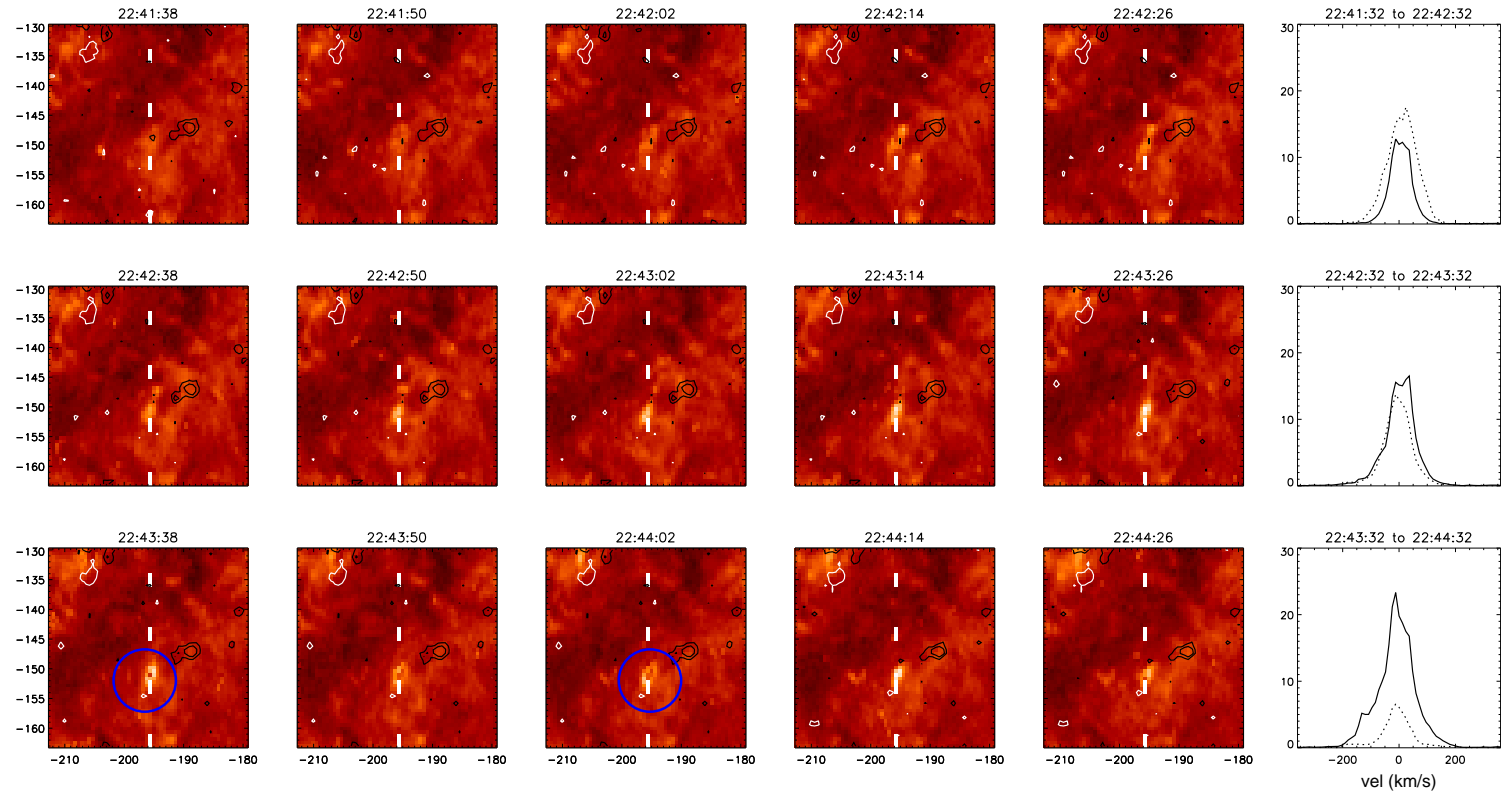


Figure 5.: Corresponding AIA images at 304Å of explosive events shown in Figure 4. The spectra on the right have been replaced by line profiles across the events. The dashed line profile is from the upper event and the solid line is from the lower one. Blue circles on the bottom row surround the ‘splash’.

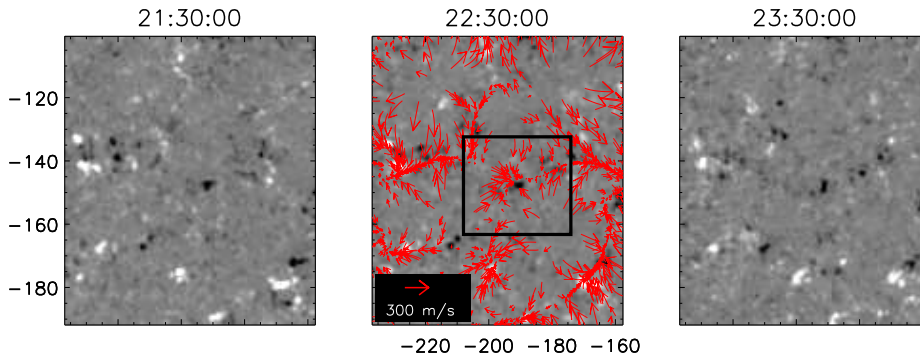


Figure 6. SDO/HMI line-of-sight magnetograms for one hour before, at the time of, and one hour after event ‘1’. The supergranular flows are overplotted as red arrows on the central image. The black rectangle surrounds the explosive event site. The magnetic field is scaled ± 50 G.

To determine the speed of the front, we constructed a time series of 171\AA base difference images along the white arrow in Figure 9. The front speed across the supergranule cell was 20 km s^{-1} (Figure 10). Waves with velocity $20\text{--}40 \text{ km s}^{-1}$, emanating from explosive event sites and crossing neighbouring supergranular cells were picked up by previous TRACE and SUMER co-observations (Innes, 2001). In that study the waves showed up in SUMER density sensitive line ratios not in the filter images so they may not be exactly the same phenomena as the front observed here but the signs are that explosive events commonly give rise to larger-scale waves and propagating fronts. Therefore we believe explosive events are signatures of plasma jets at the base of eruptions, not the moving front which explains why they do not move along the slit.

4. Summary

This is the first analysis of simultaneous explosive event and SDO imaging observations. Each event or burst of events have their own unique characteristics but all explosive events were associated with brightening in 304\AA images. They appear to be from quasi-stationary jet-like flows and are not due to the rapid rotation of spicules. Bursts of explosive events are most commonly found at mixed-polarity junctions of supergranular cells. A small region of flux emergence was also the site of multiple explosive events but this region could not be studied due to a defect on the SUMER detector. We have investigated one pair of explosive events and two explosive event bursts.

The pair of explosive events seem to have been produced by flow along a loop. Both explosive event sites appeared simultaneously in EUV channels but the

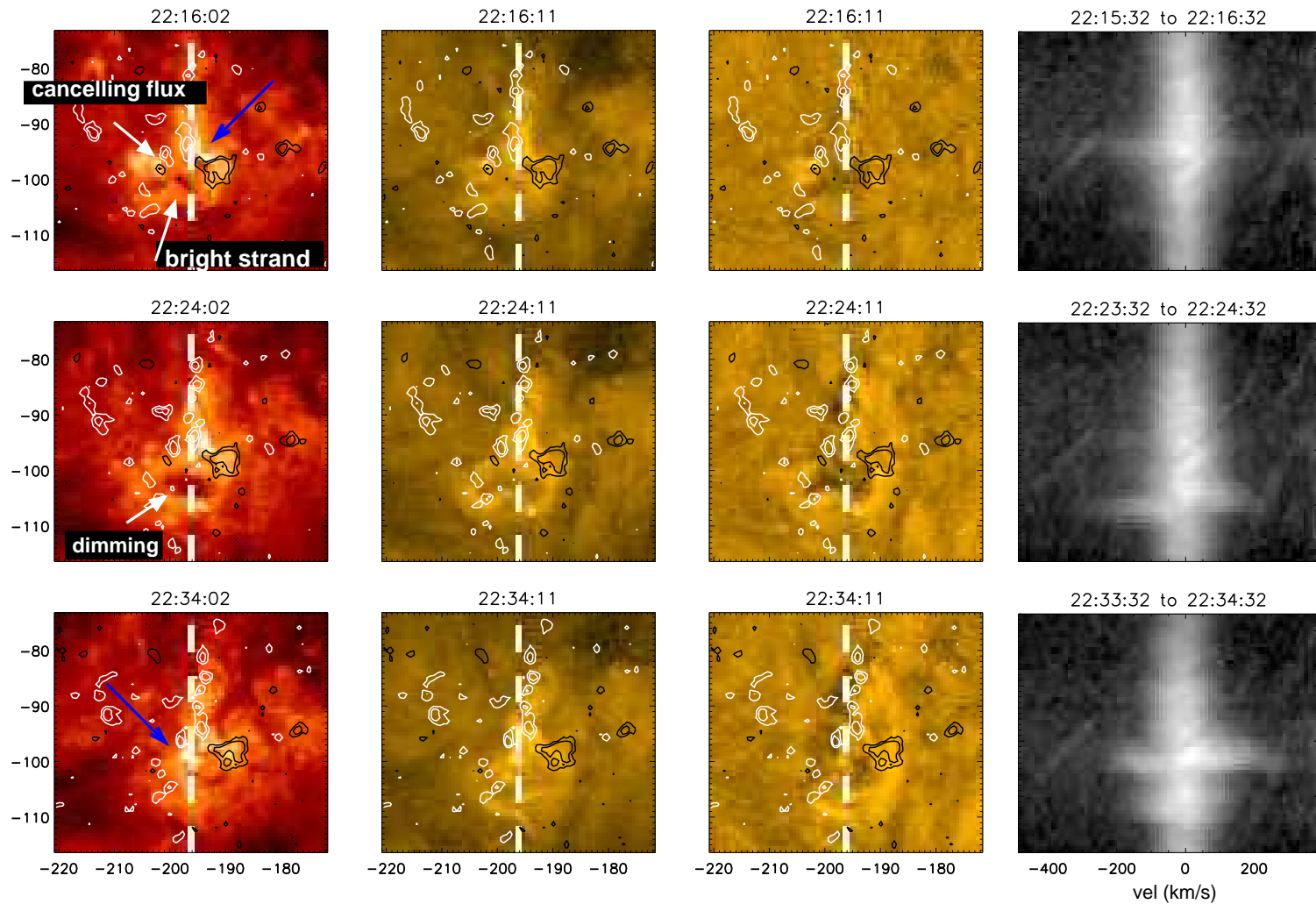


Figure 7.: Structure of sites around events ‘2’: (left-to-right) SDO/AIA 304, 171, and base difference 171Å images taken mid-way through the 60 s SUMER exposure on the right. The base difference is intensity difference between the 171Å image and an image taken 5 min before the event (i.e. at 22:10 UT). Magnetic contours at $\pm 20, 50$ G are overplotted in white/black. Blue arrows point to bright emission sites of explosive events.

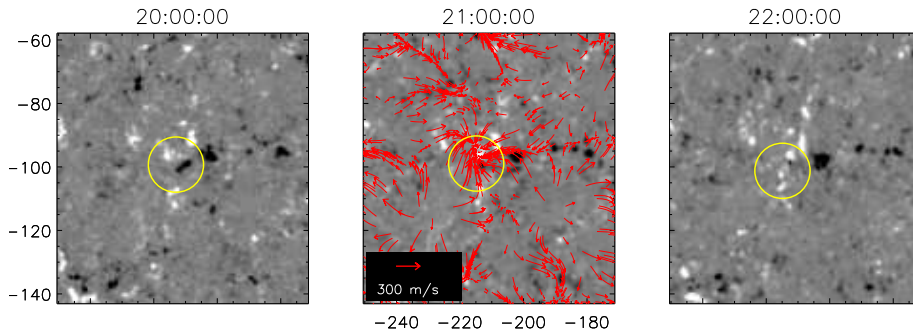


Figure 8. SDO/HMI line-of-sight magnetograms leading up to the burst of events ‘2’. The supergranular flows are overplotted as red arrows on the central image. The yellow circle surrounds cancelling flux. The magnetic field is scaled ± 50 G.

time lag of 60 s between their peak brightness and the delay between explosive events suggests that energy released at one footpoint drove a flow along the loop to the other footpoint where there was a second explosive event. The structure of the 304 and 171Å emission at the site of the second event revealed a hot core surrounded by a ring of chromospheric emission. Such a structure at the site of an explosive event has so far not been reported. We interpret it as a splash in which the explosive event is the downward and reverse jet. Alternatively, it could be the response of the lower atmosphere to a small-scale spicule-like ejection that later falls back to the surface.

Both explosive event bursts investigated here were associated with coronal dimming, implying that the coronal parts of the loops erupted. It is very likely that explosive events are bi-directional plasma jets at the footpoint of loops and these are tied to the photosphere explaining why explosive event sites do not move across the surface. This is consistent with the co-ordinated H α , 171Å, and SUMER observations of a surge (Madjarska, Doyle, and de Pontieu, 2009) which showed strong stationary explosive events co-incident with 171Å brightening at the footpoints of H α jets.

We have seen that eruptions associated with explosive events can be significantly larger than the explosive events themselves. Similar flows around explosive event sites were noted by Teriaca *et al.* (2004). When deducing the energy of the events the full extent of eruptions must be considered. This will be the topic of future studies.

Acknowledgements The authors thank the referee for critical and helpful comments. We would also like to thank R. Attie and A. Genetelli for discussion on the balltracking method. We are indebted to the SDO/AIA teams and the German Data Center at MPS for providing the data. The SUMER project is financially supported by DARA, CNES, NASA and the ESA PRODEX programme (Swiss contribution).

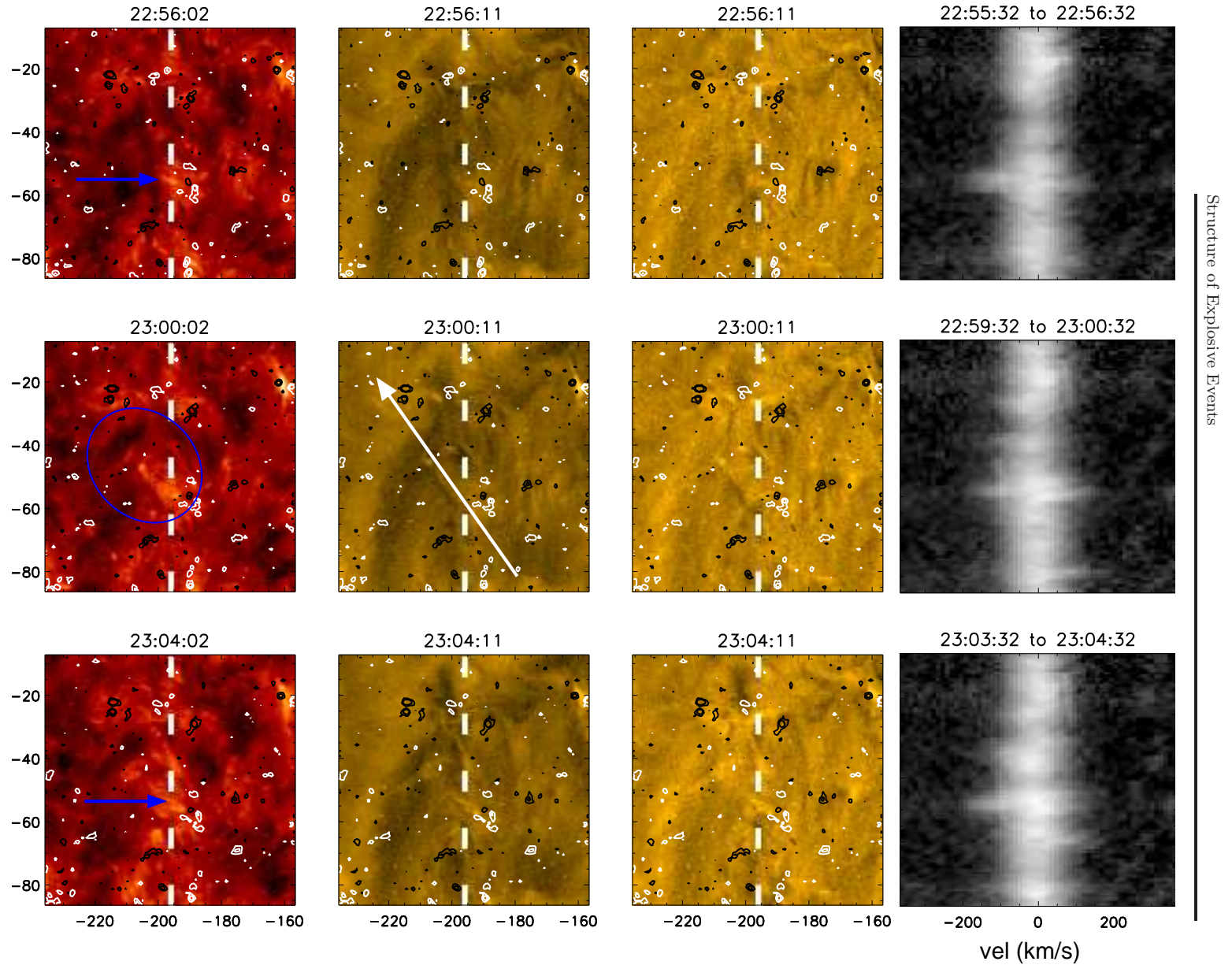


Figure 9.: Structure of sites around events ‘3’: (left-to-right) SDO/AIA 304, 171, and base difference 171Å images taken mid-way through the 60 s SUMER exposure on the right. The base difference is intensity difference between the 171Å image and an image taken 5 min before the event (i.e. at 22:50 UT). Magnetic contours at $\pm 20, 50$ G are overplotted in white/black. The white arrow shows the direction and position of the time evolution shown in Figure 10. Blue arrows point to the sites of explosive events. The blue circle surrounds the mini-CME eruption.

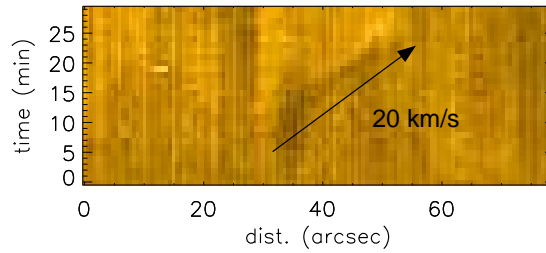


Figure 10. 171Å base difference evolution along white arrow in Figure 9.

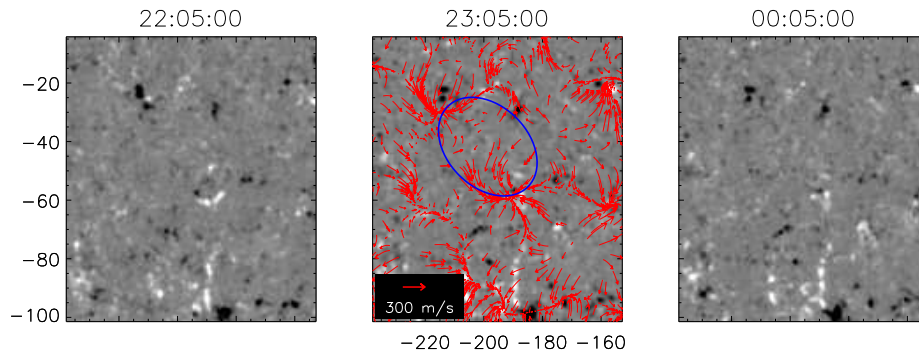


Figure 11. SDO/HMI line-of-sight magnetograms for one hour before, at the time of, and one hour after event ‘3’. The supergranular flows are overplotted as red arrows on the central image. The blue circle indicates the region affected by the eruption.

References

- Aiouaz, T.: 2008, Evidence of Relentless Reconnections at Boundaries of Supergranular Network Lanes in Quiet Sun and Coronal Hole. *Astrophys. J.* **674**, 1144–1152. doi:10.1086/524029.
- Attie, R., Innes, D.E., Potts, H.E.: 2009, Evidence of photospheric vortex flows at supergranular junctions observed by FG/SOT (Hinode). *Astron. Astrophys.* **493**, L13–L16. doi:10.1051/0004-6361:200811258.
- Brković, A., Peter, H.: 2004, Statistical comparison of transition region blinkers and explosive events. *Astron. Astrophys.* **422**, 709–716. doi:10.1051/0004-6361:20040479.
- Brueckner, G.E., Bartoe, J.-D.F.: 1983, Observations of high-energy jets in the corona above the quiet sun, the heating of the corona, and the acceleration of the solar wind. *Astrophys. J.* **272**, 329–348.
- Chae, J., Wang, H., Lee, C., Goode, P.R., Schühle, U.: 1998, Photospheric magnetic field changes associated with transition region explosive events. *Astrophys. J. Lett.* **497**, L109.
- Curd, W., Tian, H.: 2011, Spectroscopic evidence for helicity in explosive events. *Astron. Astrophys.* **532**, L9. doi:10.1051/0004-6361/201117116.
- De Pontieu, B., McIntosh, S.W., Carlsson, M., Hansteen, V.H., Tarbell, T.D., Boerner, P., Martinez-Sykora, J., Schrijver, C.J., Title, A.M.: 2011, The Origins of Hot Plasma in the Solar Corona. *Science* **331**, -. doi:10.1126/science.1197738.

- De Pontieu, B., Carlsson, M., Rouppe van der Voort, L.H.M., Rutten, R.J., Hansteen, V.H., Watanabe, H.: 2012, Ubiquitous Torsional Motions in Type II Spicules. *Astrophys. J. Lett.* **752**, L12. doi:10.1088/2041-8205/752/1/L12.
- Dere, K.P.: 1994, Explosive events, magnetic reconnection, and coronal heating. *Advances in Space Research* **14**, –.
- Dere, K.P., Bartoe, J.-D.F., Brueckner, G.E.: 1989, Explosive events in the solar transition zone. *Solar Phys.* **123**, 41–68.
- Dere, K.P., Bartoe, J.-D.F., Brueckner, G.E., Ewing, J., Lund, P.: 1991, Explosive events and magnetic reconnection in the solar atmosphere. *J. Geophys. Res.* **96**, 9399–9407.
- Doyle, J.G., Roussev, I.I., Madjarska, M.S.: 2004, New insight into the blinker phenomenon and the dynamics of the solar transition region. *Astron. Astrophys.* **418**, L9–L12. doi:10.1051/0004-6361:20040104.
- Harrison, R.A.: 1997, Euv blinkers: The significance of variations in the extreme ultraviolet quiet sun. *Solar Phys.* **175**, 467–485.
- Harrison, R.A., Lang, J., Brooks, D.H., Innes, D.E.: 1999, A study of extreme ultraviolet blinker activity. *Astron. Astrophys.* **351**, 1115–1132.
- Harrison, R.A., Harra, L.K., Brković, A., Parnell, C.E.: 2003, A study of the unification of quiet-Sun transient-event phenomena. *Astron. Astrophys.* **409**, 755–764.
- Innes, D.E.: 2001, Coordinated observations of the quiet Sun transition region using SUMER spectra, TRACE images and MDI magnetograms. *Astron. Astrophys.* **378**, 1067–1077.
- Innes, D.E., Tóth, G.: 1999, Simulations of small-scale explosive events on the sun. *Solar Phys.* **185**, 127–141.
- Innes, D.E., Inhester, B., Axford, W.I., Wilhelm, K.: 1997a, Bi-directional plasma jets produced by magnetic reconnection on the Sun. *Nature* **386**, 811–813. doi:10.1038/386811a0.
- Innes, D.E., Brekke, P., Germerott, D., Wilhelm, K.: 1997b, Bursts of Explosive Events in the Solar Network. *Solar Phys.* **175**, 341–348. doi:10.1023/A:1004997501594.
- Innes, D.E., Genetelli, A., Attie, R., Potts, H.E.: 2009, Quiet Sun mini-coronal mass ejections activated by supergranular flows. *Astron. Astrophys.* **495**, 319. doi:10.1051/0004-6361:200811011.
- Kamio, S., Curdt, W., Teriaca, L., Inhester, B., Solanki, S.K.: 2010, Observations of a rotating macrospicule associated with an X-ray jet. *Astron. Astrophys.* **510**, L1. doi:10.1051/0004-6361/200913269.
- Krucker, S., Benz, A.O.: 2000, Are heating events in the quiet solar corona small flares? multiwavelength observations of individual events. *Solar Phys.* **191**, 341–358.
- Lemaire, P., Wilhelm, K., Curdt, W., Schüle, U., Marsch, E., Poland, A.I., Jordan, S.D., Thomas, R.J., Hassler, D.M., Vial, J.-C., Kuhne, M., Huber, M.C.E., Siegmund, O.H.W., Gabriel, A., Timothy, J.G., Grewing, M.: 1997, First results of the sumer telescope and spectrometer on soho - ii. imagery and data management. *Solar Phys.* **170**, 105–122.
- Lemen, J.R., Title, A.M., Akin, D.J., Boerner, P.F., Chou, C., Drake, J.F., Duncan, D.W., Edwards, C.G., Friedlaender, F.M., Heyman, G.F., Hurlburt, N.E., Katz, N.L., Kushner, G.D., Levay, M., Lindgren, R.W., Mathur, D.P., McFeaters, E.L., Mitchell, S., Rehse, R.A., Schrijver, C.J., Springer, L.A., Stern, R.A., Tarbell, T.D., Wuelser, J.-P., Wolfson, C.J., Yanari, C., Bookbinder, J.A., Cheimets, P.N., Caldwell, D., Deluca, E.E., Gates, R., Golub, L., Park, S., Podgorski, W.A., Bush, R.I., Scherrer, P.H., Gummie, M.A., Smith, P., Auken, G., Jerram, P., Pool, P., Soufli, R., Windt, D.L., Beardsley, S., Clapp, M., Lang, J., Waltham, N.: 2012, The Atmospheric Imaging Assembly (AIA) on the Solar Dynamics Observatory (SDO). *Solar Phys.* **275**, 17–40. doi:10.1007/s11207-011-9776-8.
- Liu, Y., Hoeksema, J.T., Scherrer, P.H., Schou, J., Couvidat, S., Bush, R.I., Duvall, T.L., Hayashi, K., Sun, X., Zhao, X.: 2012, Comparison of Line-of-Sight Magnetograms Taken by the Solar Dynamics Observatory/Helioseismic and Magnetic Imager and Solar and Heliospheric Observatory/Michelson Doppler Imager. *Solar Phys.* **279**, 295–316. doi:10.1007/s11207-012-9976-x.
- Madjarska, M.S., Doyle, J.G.: 2003, Simultaneous observations of solar transition region blinkers and explosive events by SUMER, CDS and BBSO. Are blinkers, explosive events and spicules the same phenomenon? *Astron. Astrophys.* **403**, 731–741.
- Madjarska, M.S., Doyle, J.G., de Pontieu, B.: 2009, Explosive Events Associated with a Surge. *Astrophys. J.* **701**, 253–259. doi:10.1088/0004-637X/701/1/253.
- Mendoza-Torres, J.E., Torres-Papaqui, J.P., Wilhelm, K.: 2005, Explosive events in the solar atmosphere seen in extreme-ultraviolet emission lines. *Astron. Astrophys.* **431**, 339–344. doi:10.1051/0004-6361:20041299.

- Muglach, K.: 2008, Explosive Events and the Evolution of the Photospheric Magnetic Field. *Astrophys. J.* **687**, 1398–1405. doi:10.1086/592065.
- Ning, Z., Innes, D.E., Solanki, S.K.: 2004, Line profile characteristics of solar explosive event bursts. *Astron. Astrophys.* **419**, 1141. doi:10.1051/0004-6361:20034499.
- Pike, C.D., Mason, H.E.: 1998, Rotating Transition Region Features Observed with the SOHO Coronal Diagnostic Spectrometer. *Solar Phys.* **182**, 333–348.
- Podladchikova, O., Vourlidas, A., Van der Linden, R.A.M., Wülser, J., Patsourakos, S.: 2010, Extreme Ultraviolet Observations and Analysis of Micro-Eruptions and Their Associated Coronal Waves. *Astrophys. J.* **709**, 369–376. doi:10.1088/0004-637X/709/1/369.
- Porter, J.G., Dere, K.P.: 1991, The magnetic network location of explosive events observed in the solar transition region. *Astrophys. J.* **370**, 775–778.
- Potts, H.E., Barrett, R.K., Diver, D.A.: 2004, Balltracking: An highly efficient method for tracking flow fields. *Astron. Astrophys.* **424**, 253–262. doi:10.1051/0004-6361:20035891.
- Potts, H.E., Khan, J.I., Diver, D.A.: 2007, Small-Scale Energy Release Driven by Supergranular Flows on the Quiet Sun. *Solar Phys.* **245**, 55–68. doi:10.1007/s11207-007-9021-7.
- Priest, E.R., Hood, A.W., Bewsher, D.: 2002, The Nature of Blinkers and the Solar Transition Region. *Solar Phys.* **205**, 249–264.
- Roussev, I., Doyle, J.G., Galsgaard, K., Erdélyi, R.: 2001, Modelling of solar explosive events in 2D environments. III. Observable consequences. *Astron. Astrophys.* **380**, 719–726.
- Ryutova, M.P., Tarbell, T.D.: 2000, On the transition region explosive events. *Astrophys. J. Lett.* **541**, L29–L32.
- Scherrer, P.H., Schou, J., Bush, R.I., Kosovichev, A.G., Bogart, R.S., Hoeksema, J.T., Liu, Y., Duvall, T.L., Zhao, J., Title, A.M., Schrijver, C.J., Tarbell, T.D., Tomczyk, S.: 2012, The Helioseismic and Magnetic Imager (HMI) Investigation for the Solar Dynamics Observatory (SDO). *Solar Phys.* **275**, 207–227. doi:10.1007/s11207-011-9834-2.
- Scullion, E., Popescu, M.D., Banerjee, D., Doyle, J.G., Erdélyi, R.: 2009, Jets in Polar Coronal Holes. *Astrophys. J.* **704**, 1385–1395. doi:10.1088/0004-637X/704/2/1385.
- Shimojo, M., Narukage, N., Kano, R., Sakao, T., Tsuneta, S., Shibasaki, K., Cirtain, J.W., Lundquist, L.L., Reeves, K.K., Savcheva, A.: 2007, Fine Structures of Solar X-Ray Jets Observed with the X-Ray Telescope aboard Hinode. *Pub. Astron. Soc. Japan* **59**, 745.
- Sterling, A.C., Shibata, K., Mariska, J.T.: 1993, Solar chromospheric and transition region response to energy deposition in the middle and upper chromosphere. *Astrophys. J.* **407**, 778–789.
- Sterling, A.C., Mariska, J.T., Shibata, K., Suematsu, Y.: 1991, Numerical simulations of microflare evolution in the solar transition region and corona. *Astrophys. J.* **381**, 313–322. doi:10.1086/170653.
- Strong, K.T., Harvey, K., Hirayama, T., Nitta, N., Shimizu, T., Tsuneta, S.: 1992, Observations of the variability of coronal bright points by the Soft X-ray Telescope on YOHKOH. *Pub. Astron. Soc. Japan* **44**, L161–L166.
- Subramanian, S., Madjarska, M.S., Maclean, R.C., Doyle, J.G., Bewsher, D.: 2008, Magnetic topology of blinkers. *Astron. Astrophys.* **488**, 323–329. doi:10.1051/0004-6361:20079315.
- Suematsu, Y., Ichimoto, K., Katsukawa, Y., Shimizu, T., Okamoto, T., Tsuneta, S., Tarbell, T., Shine, R.A.: 2008, High Resolution Observations of Spicules with Hinode/SOT. In: Matthews, S.A., Davis, J.M., Harra, L.K. (eds.) *First Results From Hinode*, *Astronomical Society of the Pacific Conference Series* **397**, 27.
- Tarbell, T., Ryutova, M., Covington, J., Fludra, A.: 1999, Heating and Jet Formation by Hydrodynamic Cumulation in the Solar Atmosphere. *Astrophys. J. Lett.* **514**, L47–L51.
- Teriaca, L., Banerjee, D., Falchi, A., Doyle, J.G., Madjarska, M.S.: 2004, Transition region small-scale dynamics as seen by SUMER on SOHO. *Astron. Astrophys.* **427**, 1065. doi:10.1051/0004-6361:20040503.
- Wilhelm, K.: 2000, Solar spicules and macrospicules observed by SUMER. *Astron. Astrophys.* **360**, 351–362.
- Wilhelm, K., Curdt, W., Marsch, E., Schühle, U., Lemaire, P., Gabriel, A., Vial, J.-C., Grewing, M., Huber, M.C.E., Jordan, S.D., Poland, A.I., Thomas, R.J., Kuhne, M., Timothy, J.G., Hassler, D.M., Siegmund, O.H.W.: 1995, Sumer - solar ultraviolet measurements of emitted radiation. *Solar Phys.* **162**, 189.
- Wilhelm, K., Lemaire, P., Curdt, W., Schühle, U., Marsch, E., Poland, A.I., Jordan, S.D., Thomas, R.J., Hassler, D.M., Huber, M.C.E., Vial, J.-C., Kuhne, M., Siegmund, O.H.W., Gabriel, A., Timothy, J.G., Grewing, M., Feldman, U., Hollandt, J., Brekke, P.: 1997, First Results of the SUMER Telescope and Spectrometer on SOHO - I. Spectra and Spectroradiometry. *Solar Phys.* **170**, 75–104.

- Wilhelm, K., Marsch, E., Dwivedi, B.N., Feldman, U.: 2007, Observations of the Sun at Vacuum-Ultraviolet Wavelengths from Space. Part II: Results and Interpretations. *Space Sci. Rev.* **133**, 103–179. doi:10.1007/s11214-007-9285-0.
- Winebarger, A.R., Emslie, A.G., Mariska, J.T., Warren, H.P.: 2002, Energetics of Explosive Events Observed with SUMER. *Astrophys. J.* **565**, 1298–1311.
- Xia, L.D., Popescu, M.D., Doyle, J.G., Giannikakis, J.: 2005, Time series study of EUV spicules observed by SUMER/SoHO. *Astron. Astrophys.* **438**, 1115–1122. doi:10.1051/0004-6361:20042579.
- Zheng, R., Jiang, Y., Hong, J., Yang, J., Bi, Y., Yang, L., Yang, D.: 2011, A Possible Detection of a Fast-mode Extreme Ultraviolet Wave Associated with a Mini Coronal Mass Ejection Observed by the Solar Dynamics Observatory. *Astrophys. J. Lett.* **739**, L39. doi:10.1088/2041-8205/739/2/L39.

